PHYSICAL REVIEW B VOLUME 27, NUMBER 5 1 MARCH 1983

Cubic Ising lattices with four-spin interactions

O. G. Mouritsen*
Department of Physics, University of British Columbia, Vancouver, British Columbia, V6T 1W5 Canada

B. Frank
Department of Physics, Concordia University, Montreal, Quebec, H3G 1M8 Canada

D. Mukamel
Department of Nuclear Physics, The Weizmann Institute of Science, Rehovot 76100, Israel
(Received 29 April 1982; revised manuscript received 11 August 1982)

An exact derivation is given of the magnetic ground states for spin-$\frac{1}{2}$ Ising models with pure four-spin interactions on the cubic lattices. The ordered states encompass ferromagnetic, antiferromagnetic, and ferrimagnetic degenerate components, and the order-parameter dimensionality is $n=8$, 4, and ∞ for the sc, the bcc, and the fcc lattices. The Landau-Ginzburg-Wilson Hamiltonians are derived for the sc and bcc lattices. Monte Carlo calculations demonstrate that the phase transition in all three lattices is of first order. The effects of a symmetry-breaking field are investigated for the bcc lattice. The phase diagram is calculated and shown to include lines of first-order and continuous transitions as well as critical end points. The results are compared with mean-field and renormalization-group predictions.

I. INTRODUCTION

Phase transitions and critical phenomena of Ising models with multispin interactions is a topic attracting current interest since effects may be discovered that are excluded when the conventional pair-interaction approximation is applied. Furthermore, models with multispin interactions may serve as useful microscopic models for systems with complicated magnetic ground states that otherwise can only be produced by using rather exotic position-space and spin-space anisotropic pair interactions. Often, symmetry considerations rule out these latter complications and higher-order interactions must be invoked, as, e.g., in the case of the magnetic phase of solid ^{3}He.[1]

Much attention has been paid to *two*-dimensional Ising models with three- and four-spin interactions[2–8] to investigate whether nonuniversal behavior may result as in the exactly solvable Baxter model,[9] where the critical exponents vary continuously with the ratio of the two- and four-spin interaction strengths. The theoretical analyses of *three*-dimensional discrete Ising models with mixtures of pair and multispin interactions have been carried out using series expansion techniques,[10–16] Frank-Mitran theory,[17–19] mean-field theory,[20] and Monte Carlo (MC) numerical simulations.[19,21,22] Various field-theoretical continuum approximations to three-dimensional Ising models have also been investigated by renormalization group (RG) analysis.[23]

In this paper we consider three-dimensional cubic Ising lattices with interactions of the type

$$H=-J_2\sum_{\{i,j\}}\sigma_i\sigma_j-J_4\sum_{\{i,j,k,l,\}}\sigma_i\sigma_j\sigma_k\sigma_l\ . \tag{1.1}$$

$J_2>0$ and $J_4>0$ are coupling constants, and $\sigma_i=\pm1$ is the Ising spin variable associated with the ith lattice site. The first sum in Eq. (1.1) runs over all distinct nearest-neighbor pairs $\{i,j\}$ in the lattice, and the second sum comprises the simplest, distinct but geometrically equivalent four-spin clusters $\{i,j,k,l\}$ that can be embedded in the lattice under consideration. We refer to these four-spin clusters as the *basic quartets*.

In a series of papers on low-temperature series analysis,[10–14] Griffiths and Wood treated the bcc and fcc lattices with pure four-spin interactions as well as mixtures of two- and four-spin interactions. By assuming the transition to be continuous and by analyzing the critical singularities in terms of power laws, these authors argued that the pure four-spin interaction limit represents a universality class different from the $n=1$ Ising universality class, and

that the encountered variation of the critical exponents as a function of J_4/J_2 indicates nonuniversal behavior. The results obviously conflict with the universality hypothesis since the models do not fulfill the Kadanoff-Wegner criterion.[14] This puzzle was resolved recently for the fcc lattice[22] where MC calculations revealed a tricritical point and a crossover to first-order transitions for sufficiently large values of J_4/J_2. Thus the nonuniversal behavior is an artifact of the series analysis. A similar behavior has been inferred for the other two cubic lattices on the basis of a modified mean-field theory argument.[19] From a conjecture based on the Frank-Mitran theory, a scaled phase diagram was presented in Ref. 19 demonstrating the phase diagram to be almost identical for the three lattices, thereby indicating that an effective lattice-lattice scaling is present with respect to the phase behavior. The existence of a tricritical point is also supported by mean-field calculations, RG analysis,[23,24] and a proper interpretation of the results from series analysis.[22]

In this paper we shall focus on the pure four-spin interaction limit $J_2=0$ and present evidence for the first-order nature of the transition for all three lattices. We determine the ground states exactly, discuss their symmetry, and derive the Landau-Ginzburg-Wilson (LGW) Hamiltonians for the sc and bcc lattices. Furthermore we study the effects of applying a symmetry-breaking field for the bcc lattice that has a fourfold-degenerate ground state. It is found that the resulting phase diagram is rather complex, and that its structure is in agreement with recent renormalization-group calculations.[25,26]

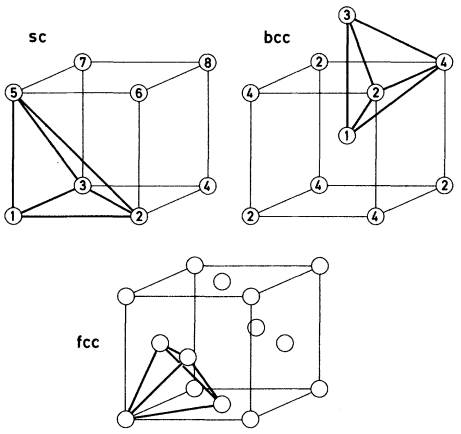

FIG. 1. Definition of the basic quartets for the three cubic lattices. The basic quartets specify the four-spin interaction in Eq. (1.1) and are indicated by the heavy solid lines. The numbers in the corners indicate the sublattice labeling employed in the ground-state analysis of Sec. II.

This paper is organized as follows: In Sec. II we give the magnetic ground states of the three lattices and derive the order-parameter index n. Also in this Section the LGW Hamiltonians for the sc and bcc lattices are presented. The phase transition is investigated in Sec. III on the basis of Monte Carlo calculations, that in Sec. IV is extended for the bcc lattice to include a symmetry-breaking field. A complete phase diagram is presented. We conclude the paper in Sec. V.

II. GROUND-STATE ANALYSIS AND LGW HAMILTONIANS

It is possible to derive exactly the magnetic ground states for the three cubic spin-$\frac{1}{2}$ lattices. As the basic quartets $\{i,j,k,l\}$ in Eq. (1.1), we choose the simplest equivalent and spatially the most confined four-spin clusters that can be embedded in the given lattice. These are indicated in Fig. 1. An important difference between the lattices is that the basic quartets for the fcc lattice involve nearest-neighbor bonds only, whereas the quartets of the sc and bcc lattices involve nearest- as well as next-nearest-neighbor bonds. Thus the ground states of the sc and bcc lattices are determined uniquely by the ground-state configuration of a single basic quartet. In contrast, for the fcc lattice a tremendous ground-state degeneracy arises. In the "ferromagnetic" case $J_4>0$, that we focus on here, a ground state for the sc and bcc lattices consists of quartets with sign combinations $(+\,+\,+\,+)$ or $(+\,+\,-\,-)$ exclusively, in contrast to the fcc lattice where a ground state may involve mixtures of the two.

The LGW Hamiltonians are presented for the sc and bcc lattices. In the case of the fcc lattice the high symmetry of the ground state precludes the construction of the corresponding LGW Hamiltonian. In the following, we present the ground-state analysis for each lattice separately and derive the index n that denotes the number of degenerate components of the corresponding order parameter.

A. sc lattice

To facilitate the analysis we define eight sublattices, labeled $1-8$ as shown in Fig. 1, and eight corresponding sublattice order parameters $\phi_1-\phi_8$. Each spin is engaged in 32 quartets.

A basic quartet couples spins from four different sublattices. When the ground-state ordering in any four sublattices, for example 1–4, is determined, the ordering in the remaining four sublattices follows uniquely in order to provide the state of lowest energy. Therefore, the following ground states occur:

$$\phi_1=\phi_2=\phi_3=\phi_4=\phi_5=\phi_6=\phi_7=\phi_8 , \tag{2.1}$$

for the ferromagnetic ground state,

$$\begin{aligned}&\phi_1=-\phi_2=\phi_3=-\phi_4=-\phi_5=\phi_6=-\phi_7=\phi_8 ,\\ &\phi_1=\phi_2=-\phi_3=-\phi_4=-\phi_5=-\phi_6=\phi_7=\phi_8 ,\\ &\phi_1=-\phi_2=-\phi_3=\phi_4=\phi_5=-\phi_6=-\phi_7=\phi_8 ,\end{aligned} \tag{2.2}$$

for the sc type-II antiferromagnetic ground state, and

$$\begin{aligned}&\phi_1=\phi_2=\phi_3=-\phi_4=\phi_5=-\phi_6=-\phi_7=-\phi_8 ,\\ &\phi_1=-\phi_2=\phi_3=\phi_4=-\phi_5=-\phi_6=\phi_7=-\phi_8 ,\\ &\phi_1=\phi_2=-\phi_3=\phi_4=-\phi_5=\phi_6=-\phi_7=-\phi_8 ,\\ &\phi_1=-\phi_2=-\phi_3=-\phi_4=\phi_5=\phi_6=\phi_7=-\phi_8 ,\end{aligned} \tag{2.3}$$

for a special antiferromagnetic ground state.

For convenience we introduce the eight intermediate order parameters

$$\begin{aligned}&\phi_1^{\pm}=\phi_1\pm\phi_8 ,\\ &\phi_2^{\pm}=\phi_2\pm\phi_7 ,\\ &\phi_3^{\pm}=\phi_3\pm\phi_6 ,\\ &\phi_4^{\pm}=\phi_4\pm\phi_5 .\end{aligned} \tag{2.4}$$

It is then evident that the ground states defined by Eqs. (2.1) and (2.2) are given as linear combinations of the ϕ_i^{+}, and the ground states in Eq. (2.3) as linear combinations of the ϕ_i^{-}. The order parameters characterizing the ground states are therefore:

$$\begin{aligned}&\psi_1=\phi_1^{+}+\phi_2^{+}+\phi_3^{+}+\phi_4^{+} ,\\ &\psi_2=\phi_1^{+}-\phi_2^{+}+\phi_3^{+}-\phi_4^{+} ,\\ &\psi_3=\phi_1^{+}+\phi_2^{+}-\phi_3^{+}-\phi_4^{+} ,\\ &\psi_4=\phi_1^{+}-\phi_2^{+}-\phi_3^{+}+\phi_4^{+} ,\\ &\psi_5=\phi_1^{-}+\phi_2^{-}+\phi_3^{-}-\phi_4^{-} ,\\ &\psi_6=\phi_1^{-}-\phi_2^{-}+\phi_3^{-}+\phi_4^{-} ,\\ &\psi_7=\phi_1^{-}+\phi_2^{-}-\phi_3^{-}+\phi_4^{-} ,\\ &\psi_8=\phi_1^{-}-\phi_2^{-}-\phi_3^{-}-\phi_4^{-} .\end{aligned} \tag{2.5}$$

Thus for the sc lattice, the ground state is eightfold degenerate and $n=8$.

The propagation vectors for the ground states $\psi_1-\psi_4$ are $\vec{k}_1=\vec{0}$, $\vec{k}_2=2\pi/a(\frac{1}{2},0,\frac{1}{2})$, $\vec{k}_3=2\pi/a(0,\frac{1}{2},\frac{1}{2})$, and $\vec{k}_4=2\pi/a(\frac{1}{2},\frac{1}{2},0)$, and for the ground states $\psi_5-\psi_8$ combinations of $\vec{k}=2\pi/a(\frac{1}{2},0,0)$, $2\pi/a(0,\frac{1}{2},0)$, $2\pi/a(0,0,\frac{1}{2})$, and $2\pi/a(\frac{1}{2},\frac{1}{2},\frac{1}{2})$, where a is the lattice parameter. The spin structures representing the peculiar states $\psi_5-\psi_8$ may be visualized as a special bcc two-sublattice antiferromagnetic structure where each sublattice constitutes a sc superlattice (with lattice constant $2a$) of octahedra involving seven lattice points of the original lattice and with corner sites shared with the six neighboring octahedra in the same sublattice.

In order to construct the LGW Hamiltonian we define a new set of order parameters:

$$\begin{aligned}&\eta_0=\phi_1^{+}+\phi_2^{+}+\phi_3^{+}+\phi_4^{+} ,\\ &\eta_{12}=\phi_1^{+}-\phi_2^{+}-\phi_3^{+}+\phi_4^{+} ,\\ &\eta_{13}=\phi_1^{+}-\phi_2^{+}+\phi_3^{+}-\phi_4^{+} ,\\ &\eta_{23}=\phi_1^{+}+\phi_2^{+}-\phi_3^{+}-\phi_4^{+} ,\\ &\eta_1=\phi_1^{-}-\phi_2^{-}+\phi_3^{-}-\phi_4^{-} ,\\ &\eta_2=\phi_1^{-}+\phi_2^{-}-\phi_3^{-}-\phi_4^{-} ,\\ &\eta_3=\phi_1^{-}+\phi_2^{-}+\phi_3^{-}+\phi_4^{-} ,\\ &\eta_{123}=\phi_1^{-}-\phi_2^{-}-\phi_3^{-}+\phi_4^{-} .\end{aligned} \tag{2.6}$$

Here the order parameters, for example, η_0, η_1, η_{12}, and η_{123}, are associated with $\vec{k}=\vec{0}$, $2\pi/a(\frac{1}{2},0,0)$, $2\pi/a(\frac{1}{2},\frac{1}{2},0)$, and $2\pi/a(\frac{1}{2},\frac{1}{2},\frac{1}{2})$, respectively. This definition of the order parameters simplifies the counting of the fourth-order invariants appearing in the LGW model. We find that there are seven fourth-order invariants, and the LGW Hamiltonian takes the form

$$H_{\mathrm{LGW}}=H_0(\eta)+\sum_{l=1}^{7}u_l 0_l(\eta) , \tag{2.7}$$

where $H_0(\eta)$ is the usual quadratic term and $O_l(\eta)$ are fourth-order polynomials in η defined as follows:

$$
\begin{aligned}
O_1 &= \eta_0^4 + \eta_{123}^4 + \sum_i \eta_i^4 + \sum_{i,j} \eta_{ij}^4 \ , \\
O_2 &= \eta_0^2 \sum_i \eta_i^2 + \eta_{123}^2 \sum_{i,j} \eta_{ij}^2 + \eta_{12}^2(\eta_1^2+\eta_2^2) \\
&\quad + \eta_{13}^2(\eta_1^2+\eta_3^2) + \eta_{23}^2(\eta_2^2+\eta_3^2) \ , \\
O_3 &= \eta_0^2 \sum_{i,j} \eta_{ij}^2 + \eta_{123}^2 \sum_i \eta_i^2 \\
&\quad + \sum_{\substack{i,j,k,l \\ (i,j\neq k,l)}} \eta_{ij}^2 \eta_{kl}^2 + \sum_{i\neq j} \eta_i^2 \eta_j^2 \ , \\
O_4 &= \eta_0^2 \eta_{123}^2 + \eta_1^2 \eta_{23}^2 + \eta_2^2 \eta_{13}^2 + \eta_3^2 \eta_{23}^2 \ , \\
O_5 &= \eta_0 \eta_{12} \eta_{13} \eta_{23} + \eta_{123} \eta_1 \eta_2 \eta_3 \ , \\
O_6 &= \eta_0 \sum_{i,j} \eta_{ij} \eta_i \eta_j + \eta_{123} \sum_{\substack{i,j,k \\ (k\neq i)}} \eta_{ij} \eta_{jk} \eta_j \ , \\
O_7 &= \eta_0 \eta_{123} (\eta_{12}\eta_3 + \eta_{13}\eta_2 + \eta_{23}\eta_1) \ .
\end{aligned}
\tag{2.8}
$$

We have not studied the renormalization-group recursion relations associated with the LGW Hamiltonian in Eqs. (2.7) and (2.8) since, as shown in Sec. III D, mean-field theory predicts the model to exhibit a strong first-order transition. Renormalization-group analysis in $d=4-\epsilon$ dimensions is not expected to change this prediction. However, the LGW Hamiltonian presented above constitutes the necessary starting point in case one would be interested in analyzing the model in the presence of symmetry-breaking fields.

B. bcc lattice

The bcc lattice is divided into four interpenetrating fcc sublattices labeled 1–4 as shown in Fig. 1. Each spin participates in 24 quartets. The basic quartets couple spins from each of the four sublattices, leaving us immediately with the following four ground states:

$$\phi_1 = \phi_2 = \phi_3 = \phi_4 \tag{2.9}$$

for the ferromagnetic ground state,

$$\phi_1 = \phi_2 = -\phi_3 = -\phi_4 \tag{2.10}$$

for the bcc type-I antiferromagnetic ground state, and

$$\phi_1 = -\phi_2 = \phi_3 = -\phi_4 \qquad \phi_1 = -\phi_2 = -\phi_3 = \phi_4 \tag{2.11}$$

for the bcc type-II antiferromagnetic ground state, and the four corresponding order parameters

$$
\begin{aligned}
\psi_1 &= \phi_1 + \phi_2 + \phi_3 + \phi_4 \ , \\
\psi_2 &= \phi_1 + \phi_2 - \phi_3 - \phi_4 \ , \\
\psi_3 &= \phi_1 - \phi_2 + \phi_3 - \phi_4 \ , \\
\psi_4 &= \phi_1 - \phi_2 - \phi_3 + \phi_4 \ .
\end{aligned}
\tag{2.12}
$$

Thus we have $n=4$ degenerate ground states in the bcc lattice.

The symmetry properties of the order parameter, Eq. (2.12), are the same as those associated with type-II fcc antiferromagnets.[27] The LGW Hamiltonian takes the form

$$
\begin{aligned}
H_{\mathrm{LGW}} = &-\tfrac{1}{2} r \sum_i \psi_i^2 - \tfrac{1}{2} \sum_i (\nabla \psi_i)^2 \\
&- u \sum_i \psi_i^4 - v \sum_{i\neq j} \psi_i^2 \psi_j^2 - w \psi_1 \psi_2 \psi_3 \psi_4 \ .
\end{aligned}
\tag{2.13}
$$

C. fcc lattice

It is convenient to consider the fcc lattice as built up of layers of rhomboid-shaped triangular lattices each with R "rows" and R "columns," the rows being along the x direction and the columns being along the y direction as defined in Fig. 2. This representation has been used by Danielian[28] for the fcc Ising lattice with nearest-neighbor antiferromagnetic pair interactions. A layer [denoted (1)] is shown in Fig. 2 for $R=6$, with toroidal periodic boundary

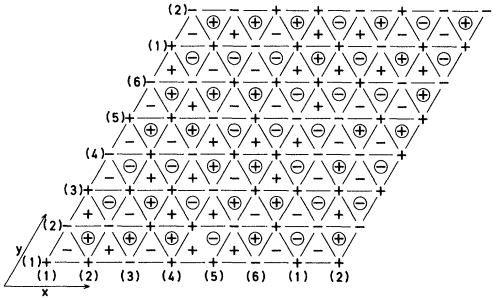

FIG. 2. Representation of three neighboring triangular layers (1)–(3) of the fcc lattice, normal to the fcc body diagonal. The layers are composed of R columns and R rows subject to periodic boundary conditions ($R=6$). The middle layer (1) consists of points connected by solid lines. The circles of centers of the triangles denote sites on layer (2) immediately below layer (1), and points at the centers of the remaining triangles denote sites on layer (3) that is immediately above layer (1). In each lattice point is placed a spin with value $\sigma_j = \pm 1$. The spin configuration given corresponds to a ground state of the model.

conditions—the circles of the centers of the triangles denote sites on layer (2) which is immediately below layer (1), and points at the centers of the remaining triangles denote sites on layer (3) which is immediately above layer (1). Each triangle of layer (1) is the base of a tetrahedron, the vertex of which is a site either on (2) or (3). Also, each site on a given layer is the vertex of two tetrahedra the bases of which are triangles on adjacent layers.

First, to determine the energy of the ground state we note that an fcc lattice of N sites can be subdivided into $2N$ tetrahedra (each site is a vertex of eight tetrahedra, and each tetrahedron has four vertices). The lowest energy possible for any tetrahedron is $-J_4$, and, as one may arrange for all tetrahedra to have energy $-J_4$ simultaneously (e.g., by having all spins with $\sigma_j=+1$), the ground-state energy for the system is $-2NJ_4$.

Moreover, there is a one-to-one correspondence between each ground state of the entire fcc lattice and the configurational state of any one of its triangular layers. This is because each site on a layer adjacent to layer (1) is the vertex of a tetrahedron the base of which is a triangle in layer (1), and therefore whatever the configuration of this triangle, the vertex (and therefore the entire adjacent layer) is determined by the ground-state requirement that each tetrahedron have an energy of $-J_4$.

We can immediately derive a relation for the ground-state degeneracy, $W\leq 2^{R^2}$, $R\sim N^{1/3}$. The equality sign would hold if each spin configuration of the triangular layer corresponded to a ground state of the entire lattice. Thus at this stage it is seen that the ground-state entropy per spin vanishes in the thermodynamic limit

$$S(T=0)/N\leq k_B R^2 \ln 2/N\rightarrow 0 \quad as \quad N\rightarrow\infty \ . \tag{2.14}$$

We now proceed to determine the degeneracy exactly. We focus our attention on clusters of eight tetrahedra consisting of a central spin on layer (1), its six nearest neighbors in layer (1) that form a hexagon, and its six neighbors in the adjacent layers (2) and (3), and ask which configurations of the seven spins ("septet") in layer (1) allow for an energy $-8J_4$ of this cluster. For so small a cluster, one can consider all the possible septet configurations in turn. As an example, Fig. 3(a) shows a septet configuration that is not consistent with the ground state. This may be seen by fixing the adjacent-layer configurations to give the ground-state energy $-J_4$ for each of the six tetrahedra with triangles in layer (1) as their bases. This is illustrated in Fig. 3(b) which shows that the energies of the two tetrahedra with the central spin as vertex have the excited value $+J_4$. The sole criterion for a given septet configuration to be consistent with the ground state of the system is

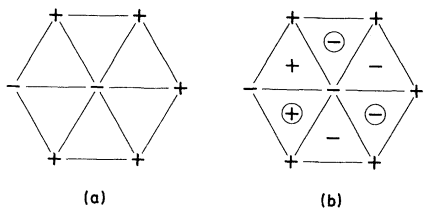

FIG. 3. Spin configuration of a cluster of eight tetrahedra, that does *not* correspond to a ground state. (a) Septet configuration of layer (1) violating Eq. (2.15). (b) Configuration on layers (1)–(3) satisfying the ground-state requirements for all tetrahedra except those with base in layer (2) or (3).

$$\prod_{i\in \text{hex}} \sigma_i=+1 \ , \tag{2.15}$$

where the product is over the sites of the six spins in layer (1) which form the hexagon of the septet.

The problem of enumerating the ground-state configurations of the fcc lattice with four-spin interactions then reduces to the following six-spin interaction problem. Consider a system of R^2 spins on a triangular lattice with the Hamiltonian

$$H_{2-d}=-J_6\sum_{j=1}^{N}\left[\prod_{i\in \text{hex}_j}\sigma_i\right] , \tag{2.16}$$

where $J_6>0$, and hex_j represents the hexagon of six spins surrounding the spin j (note, we label each hexagon by its central site). Then the degeneracy of the ground state of the fcc four-spin interaction Hamiltonian is, because of Eq. (2.15), exactly equal to the degeneracy of the ground state of H_{2-d}.

The enumeration of the ground-state configurations of the triangular lattice with six-spin interactions is accomplished by constructing upper and lower bounds for the degeneracy W. These bounds turn out to be identical in value even for finite R, and this recognition allows one to construct all ground states explicitly.

The upper bound is obtained by starting with a set of spins, called the "no-hexagon-completing" (NHC) set consisting of all spins located on the first two columns and the first row of the triangular lattice (cf. Fig. 2). For a given set of NHC spin

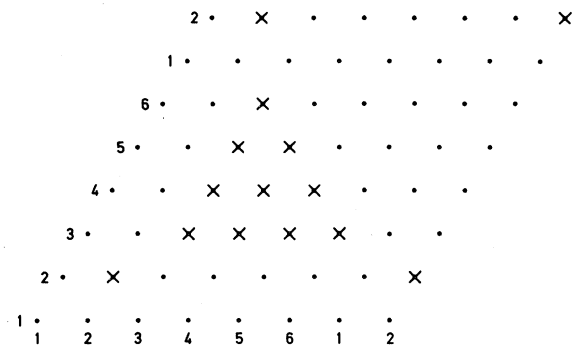

FIG. 4. Pattern of reversed spins (×) corresponding to the energy-conserving symmetry operation that reverses the (2,2) spin of the NHC set. For explanation, see Sec. II C.

values, the spins in columns 3 to R, rows 2 to R, when filled in succession, are fixed by the requirement that all hexagons they complete (and each may be taken to complete at least one hexagon) are in their ground states. Since some spins necessarily complete more than one hexagon simultaneously (due to the periodic boundary conditions), it is not obvious that any given NHC set of values leads to a ground state of the entire triangular lattice. A given NHC set of values certainly cannot lead to more than one ground state, and since there are 2^{3R-2} NHC sets of values (there being $3R-2$ spins in the set), we have

$$W \leq 2^{3R-2} , \tag{2.17}$$

that is our upper bound for W.

To find a lower bound for W, we start with the ferromagnetic ground state $\sigma_j = +1$ and we apply various symmetry operations to the spin system, consisting of spin reversals that (i) leave all hexagon configurations ($\prod_{i \in \text{hex}_j} \sigma_i$) unaltered and therefore the energy unchanged, and (ii) reverse only one spin of the $3R-2$ spins in the NHC set. We shall in this way obtain 2^{3R-2} different spin configurations each of which corresponds to a ground state of H_{2-d}. We now set up our system of symmetry operations.

For the symmetry operation satisfying (i) and (ii) that leads to the reversal of a $(j,1)$ spin ($j \geq 3$), we take the reversal of all the spins in the jth column. Reversing the sign of all the spins in any column (or row) does not change any individual hexagon index ($\prod \sigma_i$). This is so because each hexagon in the lattice involves two spins from each of the three columns (or rows) it inhabits.

For the symmetry operation that leads to the reversal of the (2,2) spin, we take the reversal of spins of the pattern described in Fig. 4 for $R=6$. For the symmetry operation that leads to the reversal of a $(2,j)$ spin ($j>2$), we take the appropriate combination of the pattern of spin reversals generated from the pattern of Fig. 4 by a translation by the vector $(0,j-2)$, and the symmetry operations previously described that lead to reversals of the $(j,1)$ spins ($j \geq 3$). For the symmetry operation that leads to the reversal of a $(1,j)$ spin ($j \geq 2$), we take the combination of a reversal of all spins in the jth row and the symmetry operations previously described that lead to the reversal of the $(2,j)$ spin. For the symmetry operation that leads to the reversal of either the (1,1) spin or the (2,1) spin, we take the reversal of all spins in column 1 or in column 2, combined with those symmetry operations considered previously, that lead in combination to the reversal of all spins $(1,j)$ ($j \neq 1$) or $(2,j)$ ($j \neq 1$), respectively.

Taking into account that, starting from the configuration with $\sigma_j + 1$ for all j, we can use our symmetry operations in combination in order to generate 2^{3R-2} distinct lattice configurations wherein each of the NHC set of $3R-2$ spins may have its $\sigma_j = \pm 1$ retaining, moreover, by condition (i) that all hexagons remain in their ground state, we conclude that

$$W \geq 2^{3R-2} . \tag{2.18}$$

Together with Eq. (2.17) we then have, exactly,

$$W = 2^{3R-2} , \tag{2.19}$$

whence

$$S(T=0) = k_B \ln W = k_B (3R-2) \ln 2 . \tag{2.20}$$

In addition we conclude that whenever we start with a given NHC set of spin values, we may construct one and only one ground state without fear that some hexagons will not "fit" when a given spin completes more than one hexagon. We stress that for the full fcc lattice also, the ground-state degeneracy is, by our reasoning above, given by Eq. (2.19). Thus not only has the number of ground-state configurations of the fcc lattice been determined, but also an explicit prescription has emerged for the construction of these configurations.

The dimensionality of the order parameter associated with this transition is given by $n = 3R-2$. This follows immediately from the above construction in that the magnetic structure is uniquely determined by the spin configuration of the NHC set, and this set has $3R-2$ linearly independent

spin configurations. The various components are found to correspond macroscopically to ferromagnetic and antiferromagnetic, as well as to ferrimagnetic spin structures.

III. PHASE TRANSITION FOR PURE FOUR-SPIN INTERACTIONS

In this section we primarily present results from MC calculations on the sc and bcc lattices. In Ref. 21 we have demonstrated for the fcc lattice with pure four-spin interactions that the phase transition is of first order associated with pronounced hysteresis effects in the internal energy and the order parameter. From the evidence presented below it is clear that the phase transition in the sc and bcc lattices is also of first order. The first-order nature of the transitions is consistent with predictions from simple Landau theory.

Using a standard MC importance sampling procedure we have calculated the temperature dependence of the internal energy per spin $E=\langle H\rangle/N$ and the n components of the order parameter

$$\psi_i = N^{-1}\left\langle \left| \sum_{j=1}^{N} \eta_j^{(i)}\sigma_j \right| \right\rangle, \quad i=1,\ldots,n \ , \tag{3.1}$$

where $\eta_j^{(i)}=\pm 1$ is a staggering index pertinent to the ith-order-parameter component. The models are arrayed on finite lattices with N spins and subjected to toroidal periodic boundary conditions. Our use of distribution functions and coarse-graining techniques, the applied convergence criteria, and the methods for detecting first-order versus continuous transitions are described in detail elsewhere.[22,29] Our results are based on statistics representing from 100 to 14 000 MCS/S, depending on whether the temperature is outside or inside transition regions (MCS/S is equal to the Monte Carlo steps per site).

A. sc lattice

Figure 5 shows the temperature dependence of the order parameter $\psi(T)$ and the normalized internal energy $E(T)/E_0$ for a system with $N=216$ spins. Two branches of the curves are observed corresponding to increasing and decreasing temperature series. Close to the termini of the branches, pronounced discontinuities are encountered for both functions. Together with the occurrence of metastable states and coexistence of phases this unequivocally demonstrates that the transition is of first order.[22] Within our observation time ($<14\,000$ MCS/S) the order on the low-temperature branch resides in one of the eight components ψ_i and the one under consideration is then termed *the* order parameter $\psi(T)$. The values of the remaining components ψ_j, $j\neq i$ are the same and small but finite due to the finite size of the lattice. On the high-temperature branch the finite-size order is distributed equally among the eight components. When the system undergoes the transition from the disordered phase to the ordered phase, it is equally likely to enter any one of the eight degenerate ordered states and the corresponding finite-temperature internal energy is found to be independent of whichever order-parameter component becomes dominant. This shows that the eightfold degeneracy is retained for all temperatures in the ordered phase.

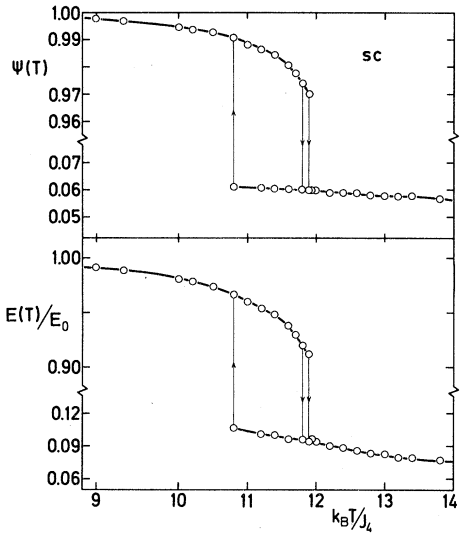

FIG. 5. Variation of order-parameter $\psi(T)$ and normalized internal energy $E(T)/E_0$ with temperature for the sc Ising lattice with pure four-spin interactions. The data points are obtained from Monte Carlo calculations on a system with $N=216$ spins. The vertical arrows indicate directions of transitions observed for increasing and decreasing temperature series.

The hysteresis loops in Fig. 5 cover an extended temperature range and it is therefore not possible directly from these static data to estimate accurately the equilibrium transition temperature. Consequently, we have performed a calculation of the lifetime τ of the metastable states in the transition region. Defining τ as the number of MCS/S to be performed before a metastable state undergoes the

transition to the stable state in course of the characteristic two-step relaxation process,[30] we have obtained the curve $\tau^{-1}(T)$ displayed in Fig. 6. A pronounced asymmetric relaxation behavior is observed and the relaxation times on the disordered metastable branch are found to be extremely long. This accords with previous observations for the fcc lattice[21] and for all three cubic lattices with mixtures of pair- and four-spin interactions.[19] The equilibrium transition temperature is the temperature where τ^{-1} attains its minimum. This leads us to the estimate $k_B T_c^{\mathrm{MC}}/J_4 = 11.4 \pm 0.3$.

Alternatively, the equilibrium transition temperature can be determined from the free-energy function $F(T)$ that in turn may be derived from the internal energy using the relationship $T\,dS = dE$. For the two phases we then have the formulas

$$F(T) = \begin{cases} E_0 + T\int_{\infty}^{1/T} [E(T) - E_0]\, d(1/T)\,, & T < T_c \quad (3.2) \\ -TS_{\infty} + T\int_{0}^{1/T} E(T)\, d(1/T)\,, & T > T_c\,, \quad (3.3) \end{cases}$$

where E_0 is the ground-state energy and $S_{\infty} = Nk \ln 2$ is the infinite-temperature entropy. In performing the integration in Eqs. (3.2) and (3.3) we use that for $k_B T/J_4 \gtrsim 12$ the MC data for $E(T)$ coalesce with the first term in the high-temperature series expansion, $E(T) = -2J_4/k_B T + \cdots$, and that deviations from E_0 are negligible for $k_B T/J_4 \lesssim 2$. The equilibrium transition temperature is obtained from the intersection point of the two free-energy branches. This leads to $k_B T_c/J_4 = 11.32 \pm 0.10$ which is consistent with the estimate from the lifetime measurements. For comparison, we quote the result for the transition temperature as obtained from the theory of Frank and Mouritsen,[19] (FM) $k_B T_c^{\mathrm{FM}}/J_4 = 12.06$. Although this theory is not strictly valid for first-order transitions, the agreement with the MC result is close.

B. bcc lattice

The MC results derived for the bcc lattice are similar to those reported above for the sc case and we therefore only give a brief account of the results. We obtain definite evidence for a first-order transition with an equilibrium transition temperature estimated from the free-energy function to be $k_B T_c/J_4 = 8.40 \pm 0.08$. This value compares favorably with the theoretical values $k_B T_c^{\mathrm{FM}}/J_4 = 8.52$ and $k_B T_c^{\mathrm{GW}}/J_4 = 8.73$ obtained from the theory of Frank and Mouritsen[19] and from the series analysis by Griffiths and Wood[11] (GW) although both of these latter approaches are not strictly valid for first-order transitions.

C. fcc lattice

The MC calculations that demonstrate that the phase transition in the fcc lattice is of first order are presented in Ref. 21, where the results are discussed in connection with a conjecture[31,11] by Wood who, on the basis of a comparison between high- and low-temperature series expansions, argued that the model is self-dual. In Ref. 21 only one phase transition is found, and the transition occurs at a temperature, $k_B T_c^*/J_4 = 2.66$, which is far above the self-dual Onsager temperature,

$$k_B T_c^O/J_2 = -2/\ln(\sqrt{2}-1) \simeq 2.27\,.$$

Therefore, the authors of Ref. 21 questioned the self-dual property of the model pointing to the infinite degeneracy of the ground state as invalidating Wood's argument. However, in the meantime two independent definite proofs have been delivered for the self-duality of the fcc lattice with pure four-spin interactions.[32,33] Therefore, in this section we discuss the status of the MC simulation of the phase transition in the fcc lattice and thus attempt a resolution of the discrepancy.

In Ref. 21, T_c^* is estimated from the terminus of the upper branches of the $E(T)$ and $\psi(T)$ curves. The position of the terminus is only weakly dependent on the lattice size. However, only for a very

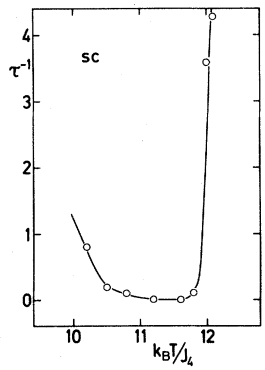

FIG. 6. Plot of inverse relaxation time τ^{-1} in arbitrary units vs temperature in the transition region for the sc Ising lattice with pure four-spin interactions. The data are obtained from Monte Carlo calculations on a system with $N = 216$ spins. A pronounced asymmetric relaxation behavior is observed.

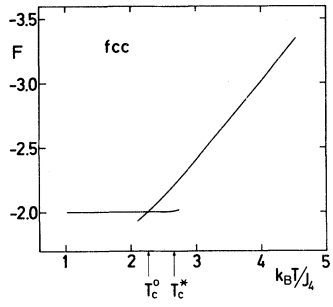

FIG. 7. Free-energy $F(T)$ vs temperature for the fcc Ising lattice with pure four-spin interactions. $F(T)$ is in units of NJ_4.

small system $N=128$ was it found possible within a reasonable number of MCS/S to make the system enter the ordered phase in the decreasing temperature series. This was interpreted as being due to the presence of metastable states with extremely long lifetimes, and the lower limit of the transition temperature was therefore estimated by using data for the $N=128$ system exclusively. Evidently, this latter procedure must be incorrect, and we have therefore undertaken a reanalysis of the MC internal energy data for the larger systems, $N=1024$ and $N=2000$, that give the same results for $E(T)$ for all temperatures and therefore presumably represent the large-N limit. Firstly, we have determined the free energy using Eqs. (3.2) and (3.3). To minimize errors in the integration procedure we have integrated in the low-T range the analytical expression for the low-temperature series expansion to order $[\exp(-4J_4/k_BT)]$[12] derived by Griffiths and Wood.[11] For $k_BT/J_4 \lesssim 2.52$ the bare series agree with the MC results within the statistical accuracy. Furthermore, we have calculated additional MC data in the high-T regime to make the data connect with the high-temperature series expansion to lowest order in $1/T$. The results for the free energy in the two phases are given in Fig. 7. From this figure the equilibrium transition temperature is found to be $k_BT_c/J_4=2.27\pm0.02$ that is precisely at the Onsager value but far below our previous estimate, 2.66. Thus a proper interpretation of the MC simulation data leads to consistency with the self-dual property of the model. Similar conclusions have recently been drawn from MC work by Liebmann[34] and Alcaraz *et al.*[35]

In Fig. 7 we see that the low-temperature free-energy curve enters the transition point almost horizontally implying that hardly any entropy is present throughout the ordered phase, e.g., at $T=T_c^-$ we have $F/J_4=-2.0024$ and the entropy contribution to F is around 1%. By contrast, the free energy at $T=T_c^+$ is strongly entropy dominated. This may explain why a small system $N=128$ exhibits a lower transition that is close to the upper one[21] simply because the small system does not possess enough microstates to produce the entropy necessary to remain at the lower branch and therefore undergoes a transition to gain internal energy. For completeness we give the discontinuity at T_c^0 of the order parameter $\Delta\psi/\psi_0=99.73\%$ as calculated from the low-temperature series.[11]

We now want to demonstrate that the Onsager transition temperature for the pure four-spin interaction model also follows from an extrapolation to $J_2=0$ of transition temperatures for models with mixtures of ferromagnetic pair interactions (J_2) and four-spin interactions [cf. Eq. (1.1)]. In Fig. 8 we present a plot of the phase diagram for this model by using a convenient set of mean-field-like scaled variables,[19]

$$\tilde{J}=\left[\frac{n_q}{n_p}\frac{J_4}{J_2}\right]\Big/\left[1+\frac{n_q}{n_p}\frac{J_4}{J_2}\right], \tag{3.4}$$

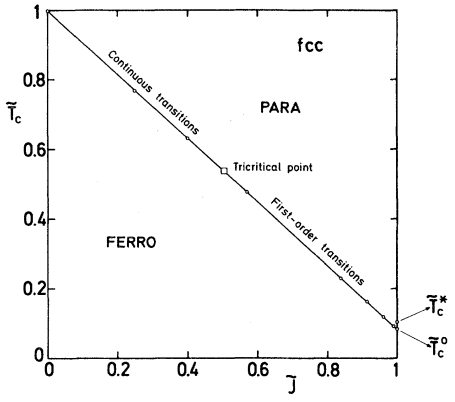

FIG. 8. Scaled phase diagram $(\tilde{J},\tilde{T}_c)$ for the fcc Ising lattice with mixtures of pair and four-spin interactions, Eq. (1.1). $\tilde{J}$ is the field variable and $\tilde{T}_c$ is the temperature variable, Eqs. (3.4) and (3.5). The diagram gives the phase boundary between the ferromagnetic and paramagnetic phases and contains a region of continuous transitions and a region of first-order transitions, separated by a tricritical point (□). The position of the tricritical point is calculated in Ref. 19 from a modified mean-field theory. ○ denotes results obtained from Monte Carlo calculations. On the right-hand axis is given the Onsager self-dual temperature $\tilde{T}_c^0$ to which the phase boundary extrapolates in the pure four-spin interaction limit, as well as $\tilde{T}_c^*$ that denotes the position of the upper transition in a system with $N=2000$ spins.

and

$$\tilde{T}_c = T_c \Big/ \left[T_c(\text{pair}) \left[J_2 + \frac{n_q}{n_p} J_4 \right] \right] . \tag{3.5}$$

n_q and n_p are the numbers of quartets and pairs that a given spin participates in, and T_c(pair) is the critical temperature in the pure pair-interaction limit expressed in units of J_2(pair), the pure-pair coupling constant. In addition to the data presented in Ref. 21, the plot of Fig. 8 contains some new points in the high-J_4/J_2 regime, that are derived for a system with $N=432$ spins. By performing an extrapolation to $\tilde{J}=1$ in this plot to determine $T_c(J_2=0)$ we circumvent any problems that may arise from the high degeneracy of the ground state in the pure four-spin interaction limit. In the scaled representation chosen, the phase boundary is linear within the statistical errors and extrapolates neatly to the Onsager self-dual temperature, T_c^O. The linear property of the phase boundary in Fig. 8 as well as an effective lattice-lattice scaling property of the three cubic lattices with mixtures of pair and quartet interactions are investigated in Ref. 19.

Before closing the section on the fcc lattice it should be mentioned that no problems with respect to determining T_c directly from $E^{\mathrm{MC}}(T)$ and $\psi^{\mathrm{MC}}(T)$ seem to have been encountered for other lattice models characterized by a high ground-state degeneracy, e.g., the fcc Ising lattice with nearest-neighbor antiferromagnetic pair interactions,[36] antiferromagnetic Potts models,[37] and Ising representations of discrete lattice-gauge theories.[38]

D. Landau theory

Taking all n ordering fields equal (denoted ϕ), the Landau free energy takes the following form for all three cubic lattices with pure four-spin interactions

$$\begin{aligned} 4F &= -n_q J_4 \phi^4 + 2k_B T[\,(1+\phi)\ln(1+\phi) \\ &\quad + (1-\phi)\ln(1-\phi)\,] \\ &= 2k_B T\phi^2 + (\tfrac{1}{3}k_B T - n_q J_4)\phi^4 + \cdots . \end{aligned} \tag{3.6}$$

This free energy leads to a first-order transition since the second-order term is positive. Thus simple Landau theory accords with our results of the MC calculations. At this point it should be emphasized that the model therefore does not probe the fluctuation-induced first-order regime studied by Kerszberg and Mukamel.[25,26]

Minimizing the free energy in Eq. (3.6) with respect to ϕ we determine the transition temperature within Landau (mean-field) theory, $k_B T_c^{\mathrm{MF}}/J_4 = 0.362\,95\, n_q$, leading to 11.61, 8.71, and 2.90 for the sc, bcc, and fcc lattices. Thus T_c^{MF} is not far above T_c^{MC}.

IV. EFFECTS OF SYMMETRY-BREAKING FIELDS. PHASE DIAGRAM FOR THE bcc LATTICE

The bcc Ising model with the $n=4$ component order parameter constitutes a useful and simple microscopic model that produces a magnetic symmetry group that attracts current attention.[26] It is of particular interest to study the influence of symmetry-breaking fields on the properties of the phase transition.[26,39] We have therefore applied a symmetry-breaking field g to the bcc Ising model with pure four-spin interactions. The field g may correspond to a magnetic field or an uniaxial stress that only couples to even orders in the order parameter. We consider symmetry-breaking fields that split the $n=4$ degeneracy into an $n=3$ and an $n=1$ representation. We wish to determine the phase diagram in the (T,g) plane.

In the microscopic Hamiltonian, g is simulated by suitable pair interactions defined on subsets of the four interpenetrating sublattices given in Fig. 1. Note that the four-spin term couples these four sublattices. Here we single out one or three sublattices by introducing ferromagnetic fcc nearest-neighbor (bcc third-nearest neighbor) interactions in the sublattices. The effective Hamiltonian then takes the form

$$\begin{aligned} H = &-J_2^+ \sum_{\{i,j\}}^{(1)} \sigma_i\sigma_j - J_2^- \sum_{\{i,j\}}^{(2+3+4)} \sigma_i\sigma_j \\ &- J_4 \sum_{\{i,j,k,l\}} \sigma_i\sigma_j\sigma_k\sigma_l, \quad J_2^+ > 0,\ J_2^- > 0 , \end{aligned} \tag{4.1}$$

where the first sum is defined on sublattice 1 and the second sum on sublattices 2–4.

In terms of the fields $\phi_1 - \phi_4$ defined in Sec. II (cf. Fig. 1), the corresponding Landau free-energy functional may be written (to fourth order in ϕ)

$$\begin{aligned} 4F = &-n_q J_4 \phi_1\phi_2\phi_3\phi_4 + 2(k_B T - n_p J_2^+)\phi_1^2 \\ &+ 2(k_B T - n_p J_2^-) \sum_{i=2}^{4} \phi_i^2 + \frac{k_B T}{3} \sum_{i=1}^{4} \phi_i^4 . \end{aligned} \tag{4.2}$$

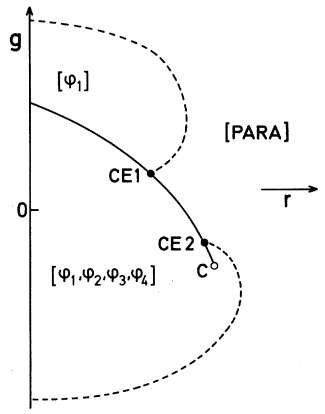

FIG. 9. Schematic phase diagram (r,g) for the model in Eq. (4.1) solved within the mean-field approximation. For small values of $|g|$ there is a first-order transition from the fourfold degenerate phase $[\phi_1,\phi_2,\phi_3,\phi_4]$ to the paramagnetic phase. For large positive values of g there is a four-state Potts-type transition within the ordered phase to the one-component phase $[\phi_1]$ that for high temperatures undergoes an $n=1$ Ising-type continuous transition to the disordered phase. For intermediate negative values of g there is also a first-order transition line inside the ordered phase. This line terminates in a liquid-gas-like critical point, C. For high temperatures there is an $n=3$ Heisenberg-type (with cubic anisotropy) transition to the paramagnetic phase. $CE1$ and $CE2$ are critical end points. First-order and continuous transition lines are given by (——) and (----), respectively.

For convenience we introduce the scaling fields r and g defined by[26]

$$g=\tfrac{1}{2}n_p(J_2^+-J_2^-)\,,$$
$$r=2k_BT-\tfrac{1}{2}n_p(J_2^++3J_2^-)\,. \qquad (4.3)$$

r is the temperaturelike variable. The mean-field phase diagram (r,g) resulting from the free energy in Eq. (4.2) has been calculated by Kerszberg and Mukamel[26] for a similar $n=4$ model and its qualitative characteristics are shown in Fig. 9. The diagram is rather complex including first-order and continuous transition lines, two critical end points, and a liquid-gas-like critical point. For low values of $|g|$ there is a single first-order transition from the fourfold degenerate phase $[\phi_1,\phi_2,\phi_3,\phi_4]$ to the paramagnetic phase. For larger values of g there is a four-state Potts-type first-order transition within the ordered phase to the one-component phase $[\phi_1]$. In this phase the fluctuations of the fields ϕ_2, ϕ_3, and ϕ_4 are quenched and for high temperatures the system undergoes an $n=1$ continuous Ising-type transition. For an intermediate range of negative values of g there is also a first-order transition within the ordered phase. The corresponding phase line, that terminates in a liquid-gas-like critical point, is not associated with a change of symmetry.[26] Since the order parameters ϕ_2, ϕ_3, and ϕ_4 induce a field $\propto\phi_2\phi_3\phi_4$ that couples linearly to ϕ_1, all four fields are nonzero on the high-temperature side of this transition. For still higher temperatures there is a line of continuous phase transitions to the paramagnetic phase. This transition line, that belongs to the universality class of the $n=3$ Heisenberg model with cubic anisotropy, persists for large negative values of g.

We have carried out MC temperature scans for a series of values of g in order to map out the phase diagram. In Fig. 10 we give, in the case of $g=1.5$ and 6, the results for the internal energy and the two types of order parameters, ψ and ϕ_1. ψ is one of the four components ψ_α, $\alpha=1,\ldots,4$, defined in Eq. (2.12). The internal energy is split into its two contributions from the pair interactions (E^p) and the four-spin interactions (E^q). For $g=1.5$ the figure shows a pronounced discontinuity in all functions implying that the phase transition is of first order. A very narrow hysteresis loop is encountered as well. For $g=6$ the behavior has drastically

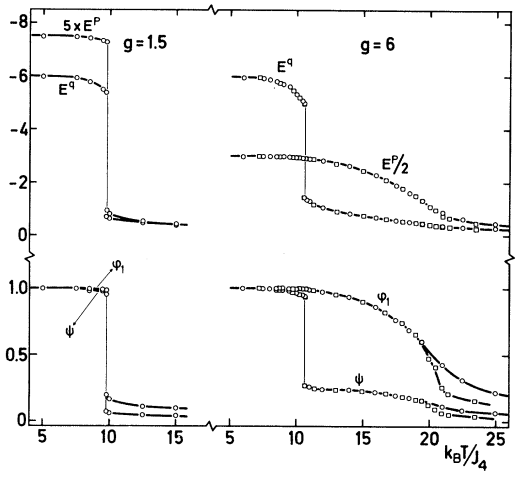

FIG. 10. Temperature dependence of internal energies and order parameters for a bcc Ising model with four-spin interactions and subjected to a positive symmetry-breaking field g [cf. Eq. (4.1)]. E^p and E^q are the pair-interaction and four-spin interaction energies. ψ is the order parameter governed by the four-spin interaction, Eq. (2.12), and ϕ_1 is the order parameter governed by the pair interaction defined in sublattice 1 (cf. Fig. 1). Monte Carlo data are given for systems with $N=432$ (○) and $N=2000$ (□) spins. All energies are in units of NJ_4. g is simulated by pair interactions with $J_2^+>0$ and $J_2^-=0$.

changed. Now we observe two consecutive transitions. The lower one is of first order signaled by discontinuities in E^q and ψ. This transition is described by an effective four-state Potts-type Hamiltonian, and our finding of a first-order transition accords with the theoretical predictions for three-dimensional Potts models with three or more components.[40]. The functions E^p and ϕ_1 pass smoothly through this first transition. At the upper transition, E^p and ϕ_1 change in a continuous manner. In going from $g=1.5$ to 6, the discontinuities in E^q and ψ decrease. In Fig. 10 the data for $g=6$ are given for two different lattice sizes, $N=432$ and 2000. We note that the lower transition is not significantly affected by finite-size effects, that is expected for a first-order transition. However, the upper transition becomes significantly more sharp but remains continuous when N is increased. ϕ_1 is more affected than E^p. Furthermore, we find that the heat capacity peak increases in intensity and moves towards higher temperatures when the lattice size is increased. All this evidence is consistent with the upper transition being continuous. However, we do not have sufficient information to determine critical exponents and thereby identify the universality class. It should be noted that only one quarter of the system goes critical at this upper transition. The order parameter ψ is nonzero in the intermediate phase because ψ via Eq. (2.12) involves ϕ_1. Therefore, also ψ decreases continuously at the upper transition, and the high-temperature tail of this order parameter, as well as that of ϕ_1, is due to conventional finite-size effects.

We now turn to negative values of the symmetry-breaking field g. For small negative g, we observe a single clear and pronounced first-order transition. In the case of larger negative g values, $g=-7.5$ and 12, Fig. 11 displays the MC results for E^p, E^q, and the order parameters ψ and $\phi=\frac{1}{3}(\phi_2+\phi_3+\phi_4)$. Data for $N=432$ and 2000 are shown, and for the sake of clarity only results for the larger system are plotted in the case of the order parameters close to and above the transition. For $g=-7.5$ simultaneous discontinuities in all four functions indicate the presence of a single first-order transition. However, for this value of g the finite-size effects are much more pronounced than for the values of g given in Fig. 10. These finite-size effects (not shown in the figure) tend to diminish the discontinuities and lead to a partial smearing of the transition. Thus we conclude that significant thermodynamic fluctuations have come to play a role and the system may not be far from a

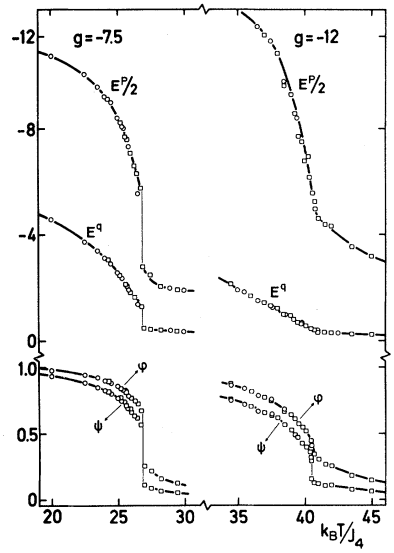

FIG. 11. Temperature dependence of internal energies and order parameters for a bcc Ising model with four-spin interactions and subjected to a negative symmetry-breaking field g [cf. Eq. (4.1)]. ψ is the order parameter governed by the four-spin interactions, and ϕ is the order parameter governed by the pair interactions defined in sublattices 2–4 (cf. Fig. 1). The remaining symbols are explained in Fig. 11. g is simulated by pair interactions with $J_2^+=0$ and $J_2^-<0$.

critical point. For $g=-12$, Fig. 11 shows that the discontinuities in E^p, ϕ, and E^q now have disappeared, but a small jump in ψ remains. The temperature and finite-size variation of E^p and ϕ show characteristics of a continuous transition, in contrast to that of ψ that definitely still undergoes a first-order transition, although E^q is now changing smoothly in the transition region. As always in numerical simulations we cannot exclude that a seemingly continuous transition is actually a first-order one with a very small discontinuity that is veiled by the finite-size effects. However, we shall here assume that the transition in E^p and ϕ is continuous. It is more important that there appears to be a separation between the two transitions indicated by the fact that the inflection point of E^p and ϕ appears slightly above the jump in ψ. Thus our data are consistent with two very close-lying transitions. This supports the mean-field phase diagram in Fig. 9. According to this diagram, the first-order line terminates, for increasing negative g values, in a critical point simultaneously with an increase of the separation between the two transitions. However, since the discontinuity in ψ decreases when the critical point is approached and since the discontinuity

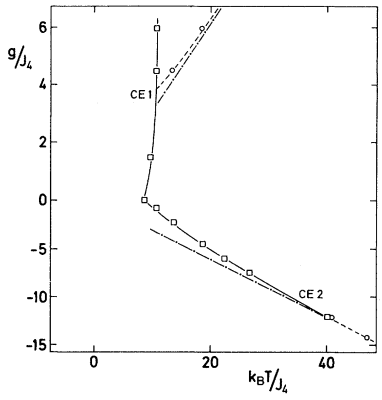

FIG. 12. Phase diagram (T,g) for the model in Eq. (4.1) as obtained from Monte Carlo calculations (cf. the mean-field phase diagram in Fig. 9). The scaling field g is defined in Eq. (4.3). □ denotes first-order transitions, ○ denotes continuous transitions, and the corresponding phase lines are indicated by solid and dashed lines, respectively. The approximate positions of the two critical end points $CE1$ and $CE2$ are also given. The dot-dash line signifies the pure pair-interaction limit for the fcc lattice.

found in the MC calculations for $g=-12$ is already close to the limit of our resolution, we have not found it fruitful to search for a more well-separated set of transitions by choosing a slightly larger negative value of g. For $g=-14.25$ we encounter only a single transition, and all quantities change smoothly in the transition region indicating that the transition is continuous.

Our complete MC information on the transitions in the model is collected in the composite phase diagram shown in Fig. 12. In terms of the variables (T,g) the diagram has a kink for $g=0$. When using the scaled variables in Eq. (4.3) this kink disappears and the phase boundary varies smoothly through $g=0$. The various phase lines are indicated and the approximate positions of the two critical end points $CE1$ and $CE2$ are indicated. The position of $CE2$ is of course rather uncertain, $-7.5 \lesssim g(CE2) \lesssim -12$. The dot-dash lines in the figure correspond to the limit of $J_2^{\pm}/J_4 \to \infty$, i.e., pure pair interactions on an fcc lattice.[41] This limit seems to have been reached effectively for $g \lesssim -14.25$.

V. CONCLUDING REMARKS

We have studied the phase behavior of Ising models with four-spin interactions defined on the cubic lattices. The magnetic ground states are derived exactly and turn out to be complicated, involving degenerate order parameters with $n=8$, 4, and ∞ components for the sc, bcc, and fcc lattices. All ground states are shown to have zero residual $(T=0)$ entropy per site. The LGW Hamiltonians have been constructed for the sc and bcc lattices. Monte Carlo simulations demonstrate that the phase transition in all three lattices is of first order, in accordance with simple mean-field and renormalization-group predictions. The results for the transition temperature of the fcc model are shown to be consistent with a self-dual property recently proved for this model. We have investigated the phase diagram for the $n=4$ bcc model with four-spin interactions in the presence of a symmetry-breaking field g. The resulting phase diagram, shown in Fig. 12, is rather complex with lines of first order and continuous transitions as well as two critical end points. The overall structure of the diagram is in agreement with renormalization-group calculations. It turns out that simple Landau (or mean-field) theory in a qualitatively correct way describes the phase diagram for this model. Although not very precise, the Monte Carlo results for the position of the critical end points in Fig. 12 are in accordance with the renormalization-group prediction for the amplitude ratio, $g(CE2)/g(CE1)=-3+O(\epsilon)$.

ACKNOWLEDGMENTS

We would like to thank A. J. Berlinsky for stimulating discussions throughout the progression of this work. R. Liebmann, P. A. Pearce, and R. J. Baxter, as well as F. C. Alcaraz, L. Jacobs, and R. Savit are thanked for sending us preprints of their work on the fcc Ising model with four-spin interactions. One of us (B.F.) acknowledges support from the Natural Sciences and Engineering Research Council of Canada. Another of us (O.G.M.) acknowledges the kind hospitality accorded him during several stays at Concordia University where part of this work was carried out, that of Professor Myer Bloom and the Physics Department of the University of British Columbia (UBC) during his sabbatical year, and support from the Danish Natural Science Research Council. One of us (D.M.) was supported in part by a grant from the Israel Academy of Sciences and Humanities—Basic Research Foundation.

*On leave of absence from Department of Physical Chemistry, Aarhus University, DK-8000 Aarhus C, Denmark.

[1]A. Landesman, J. Phys. (Paris) Colloq. C6, 1305 (1978).
[2]R. J. Baxter and F. Y. Wu, Phys. Rev. Lett. 31, 1294 (1973).
[3]J. Oitmaa and R. W. Gibberd, J. Phys. C 6, 2077 (1973); J. Oitmaa, *ibid.* 7, 389 (1974).
[4]F. Y. Wu, J. Phys. C 10, L23 (1977).
[5]K. Jüngling, J. Phys. C 9, L139 (1976).
[6]D. Imbro and P. C. Hemmer, Phys. Lett. 57A, 297 (1976).
[7]S. Frøyen, Aa. S. Sudbø, and P. C. Hemmer, Physica 85A, 399 (1976).
[8]M. Yamashita, H. Nakano, and K. Yamada, Prog. Theor. Phys. 62, 1225 (1979).
[9]R. J. Baxter, Phys. Rev. Lett. 26, 832 (1971); L. P. Kadanoff and F. J. Wegner, Phys. Rev. B 4, 3989 (1971).
[10]D. W. Wood and H. P. Griffiths, J. Math. Phys. 14, 1715 (1973).
[11]H. P. Griffiths and D. W. Wood, J. Phys. C 6, 2533 (1973).
[12]D. W. Wood and H. P. Griffiths, J. Phys. C 7, 1417 (1974).
[13]D. W. Wood and H. P. Griffiths, J. Phys. C 7, L54 (1974).
[14]H. P. Griffiths and D. W. Wood, J. Phys. C 7, 4021 (1974).
[15]J. Ho-Ting-Hun and J. Oitmaa, J. Phys. A 9, 2125 (1976).
[16]R. V. Ditzian, Phys. Lett. 42A, 67 (1972).
[17]O. Mitran, J. Phys. C 12, 557 (1979); 12, 4871 (1979); Ph.D. thesis, Concordia University, Montreal, 1979 (unpublished).
[18]B. Frank, J. Phys. C 12, L595 (1979).
[19]B. Frank and O. G. Mouritsen, J. Phys. C (in press).
[20]V. M. Matveev and E. L. Nagaev, Fiz. Tverd. Tela (Leningrad) 14, 492 (1972) [Sov. Phys.—Solid State 14, 408 (1972)].
[21]O. G. Mouritsen, S. J. Knak Jensen, and B. Frank, Phys. Rev. B 23, 976 (1981).
[22]O. G. Mouritsen, S. J. Knak Jensen, and B. Frank, Phys. Rev. B 24, 347 (1981).
[23]M. Gitterman and M. Mikulinsky, J. Phys. C 10, 4073 (1977).
[24]A. Aharony, Phys. Rev. B 9, 2416 (1974).
[25]M. Kerszberg and D. Mukamel, Phys. Rev. B 23, 3943 (1981).
[26]M. Kerszberg and D. Mukamel, Phys. Rev. B 23, 3953 (1981).
[27]D. Mukamel and D. J. Wallace, J. Phys. C 12, L851 (1979).
[28]A. Danielian, Phys. Rev. Lett. 6, 670 (1961).
[29]O. G. Mouritsen and S. J. Knak Jensen, Phys. Rev. B 18, 465 (1978).
[30]D. P. Landau and K. Binder, Phys. Rev. B 17, 2328 (1978).
[31]D. W. Wood, J. Phys. C 5, L181 (1972).
[32]R. Liebmann, Phys. Lett. 85A, 59 (1981).
[33]P. A. Pearce and R. J. Baxter, Phys. Rev. B 24, 5295 (1981).
[34]R. Liebmann, Z. Phys. B 45, 243 (1982).
[35]F. C. Alcaraz, L. Jacobs, and R. Savit, Phys. Lett. 89A, 49 (1982).
[36]M. K. Phani, J. L. Lebowitz, M. K. Kalos, and C. C. Tsai, Phys. Rev. Lett. 42, 577 (1979).
[37]J. R. Banavar, G. S. Grest, and D. Jasnow, Phys. Rev. Lett. 45, 1424 (1980).
[38]C. Rebbi, Phys. Rep. 67, 55 (1980).
[39]S. J. Knak Jensen, O. G. Mouritsen, E. Kjaersgaard Hansen, and P. Bak, Phys. Rev. B 19, 5886 (1979).
[40]R. K. P. Zia and D. J. Wallace, J. Phys. A 8, 1495 (1975).
[41]M. E. Fisher and R. J. Burford, Phys. Rev. 156, 583 (1967).